Satellite retrievals of (quasi-)spherical particles at cold temperatures

Yong-Sang Choi,[1] Chang-Hoi Ho,[2] Jinwon Kim,[3] and Richard S. Lindzen[1]

Received 18 November 2009; revised 26 January 2010; accepted 3 February 2010; published 5 March 2010.

[1] Measurements from NASA's A-train satellites indicate that spherical or quasi-spherical particles may constitute up to 30% of the total cloud particles at temperatures below −30°C, and up to 10% even for temperatures below −40°C, the temperature range typically found in the upper troposphere and the lower stratosphere. Current climate models calculate cloud radiative forcing on the basis on an assumption that essentially no spherical or quasi-spherical particles exist below −40°C (even below −15°C). The findings in this study show that this widely used assumption in climate models may need re-examination. Further research is also needed to confirm and quantify these findings, especially improvements in the satellite retrievals of cloud particle shapes that, in the mean, currently contain about 10% uncertainties. **Citation:** Choi, Y.-S., C.-H. Ho, J. Kim, and R. S. Lindzen (2010), Satellite retrievals of (quasi-)spherical particles at cold temperatures, *Geophys. Res. Lett.*, *37*, L05703, doi:10.1029/2009GL041818.

1. Introduction

[2] Cloud particle shapes are among the major factors that determine cloud radiative forcing because the radiative properties of cloud particles vary widely according to their shapes [*Liou*, 2002; *Yang et al.*, 2005]. In general, cloud particles have been categorized into spherical and non-spherical shapes [*Fu*, 1996] for calculating cloud radiative properties. Because of large differences in the radiative properties between spherical and non-spherical particles, inaccurate partitioning of cloud particle shapes can lead to systematic biases in simulating equilibrium climate [*Senior and Mitchell*, 1993; *Ho et al.*, 1998].

[3] Most radiative transfer schemes in today's climate models assume that all clouds follow radiative properties of non-spherical particles below a threshold temperature that typically ranges from −15°C to −40°C [*Del Genio et al.*, 1996]. This critical assumption is based on the conventional wisdom of cloud microphysics that (spherical) water drops coexist with (non-spherical) ice particles in clouds between −40°C and 0°C, and that water drops are rapidly glaciated (i.e., converted into non-spherical ice particles) with decreasing temperature to practically negligible amounts below −20°C [*Pruppacher and Klett*, 1997]. More sophisticated models determine cloud particle shape compositions in a complicated way by considering additional factors such as ambient humidity, the composition, contents, and size distribution of ice nuclei, and dynamical mixing of cloud particles [e.g., *Storelvmo et al.*, 2008]. Recent observational studies suggest that spherical and/or quasi-spherical cloud particles are present in significant amounts at temperatures colder than −30°C, for example, liquid-phase nitric acid compounds [*Noel et al.*, 2008], or small droxtal ice crystals [*Zhang et al.*, 2004]. This would be an important concern in calculating radiative forcing in climate models because the fundamental radiative properties of spherical or quasi-spherical particles are different from non-spherical particles [*Liou*, 2002; *Yang et al.*, 2005].

[4] This study examines the composition of cloud particle shapes according to atmospheric temperatures for the entire globe using recent spaceborne retrievals that are based on the differences in the bulk optical properties between "spherical" and non-spherical particles. It is important to note here that we group quasi-spherical ice particles with "spherical" particles in our calculation of spherical particle fraction (SPF). In other words, the retrieval processes do not distinguish between spherical and quasi-spherical particles, and there is no information to determine whether these particles are ice particles or water drops. Although the current satellite retrievals have much room for improvement, they provide an extensive volume of data on cloud fields with wide spatial and temporal coverage beyond that achievable by *in situ* measurements. We utilize the cloud particle phase/shape datasets from two different sensors onboard NASA's so-called A-train constellation, the Moderate Resolution Imaging Spectroradiometer (MODIS) and the Cloud-Aerosol Lidar with Orthogonal Polarization (CALIOP).

2. Data and Methods

[5] The MODIS/Terra gridded level-3 atmospheric data (MOD08, Collection 4) for the 7-year period, 2000–2006, have been analyzed in this study. MODIS cloud-top phase retrievals utilize infrared (IR) brightness temperatures that are available for both day and night [*Baum et al.*, 2000] on the basis of the IR-wavelength dependencies of the absorptivity of spherical (liquid) particles and non-spherical (ice) particles. The current MODIS algorithm compares the brightness temperatures at two channels (8.5- and 11-μm) and classifies cloud water into four categories such as liquid, ice, mixed, and uncertain phases [*Menzel et al.*, 2006]. Recent theoretical calculations of the single-scattering properties of ice particles [*Yang et al.*, 2005] show that the absorption efficiency of droxtals in the IR wavelengths is located between spheres and spheroids, but is far from other non-

[1]Department of Earth, Atmospheric and Planetary Sciences, Massachusetts Institute of Technology, Cambridge, Massachusetts, USA.
[2]School of Earth and Environmental Sciences, Seoul National University, Seoul, South Korea.
[3]Department of Atmospheric and Oceanic Sciences, University of California, Los Angeles, California, USA.

0094-8276/10/2009GL041818$05.00

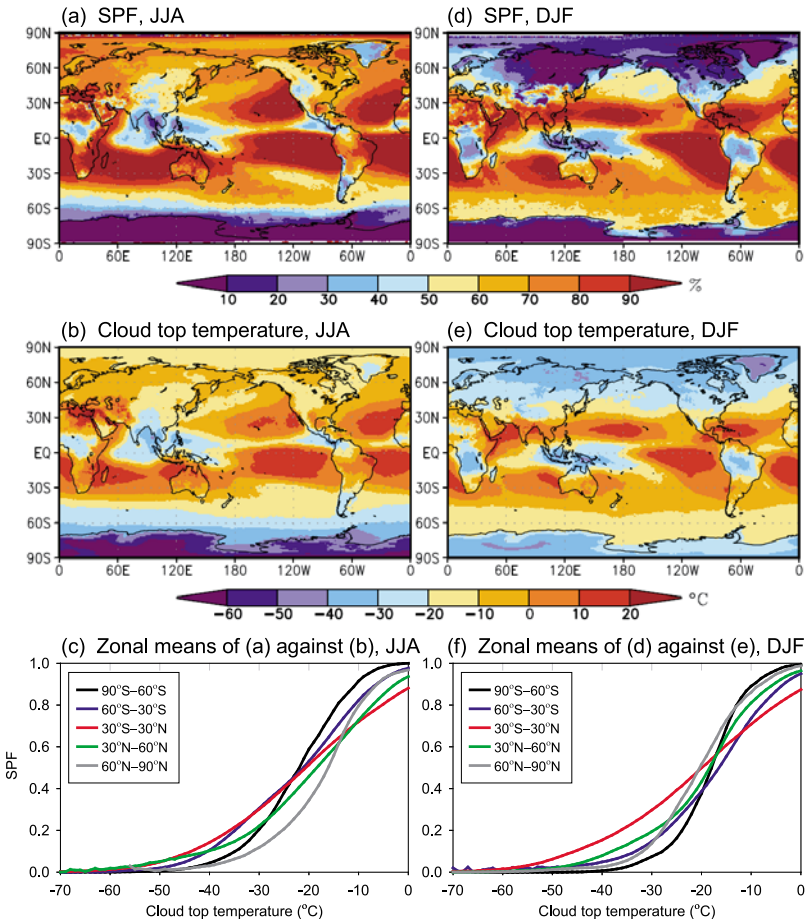

Figure 1. Global distribution of (quasi-)spherical particle fractions to the total cloud at cloud tops and cloud top temperature from the MODIS data for (a and b) June, July, and August and for (d and e) December, January, and February of 2000–2006. (c and f) Zonal mean values of spherical particle fraction and cloud top temperature are also shown for two seasons.

spherical ice habits. Thus, quasi-spherical particles can be identified as spherical particles. Moreover, the accuracy of the data is reduced by the contamination factors of the IR radiances such as absorption by atmospheric water vapor, scattering properties of clouds, surface emissivity, and cloud height [*Menzel et al.*, 2006].

[6] Additional cloud particle shape data from the CALIOP lidar level-2 vertical feature mask (version 2.01) for August 2006 and February 2007 that have the same categories as the MODIS data has also been examined to supplement the MODIS retrievals. From the surface to an altitude of 8.2 km, the horizontal and vertical resolutions of the CALIOP data are 333 m and 30 m, respectively, with coarser resolutions (1000 m and 60 m in horizontal and vertical, respectively) in the altitude range from 8.2 to 20.2 km. The CALIOP determines cloud shape largely by the layer-integrated particle depolarization ratio at 532 nm [*Liu et al.*, 2005]. The backscatter signal of a linearly polarized laser beam from the spherical particles is completely linearly polarized, i.e., the depolarization ratio ≈ 0%. If the particles are not spherical, or the measured backscattered signal is affected by multiple scattering (e.g., optically thick liquid clouds), the backscattered lidar signal contains a cross-polarized contribution; non-spherical ice crystals typically have the depolarization ratio in the range of 30%–50%. However, the frequent presence of horizontally oriented ice plates in cirrus clouds produce very low depolarization, and the algorithm falsely identifies them as spherical particles. We note that this problem is embedded in the data, but spherical particles remain considerable down to −30°C even in the updated data [*Hu et al.*, 2009].

[7] An obvious question is the reliability of cloud particle shape retrievals admitting shortcomings in the satellite observations. The two independent retrievals from MODIS and CALIOP can be compared because these two sensors receive information from the same clouds within a few second intervals. The cross-examination uses the MODIS/Aqua level-2 cloud product (MYD06, Collection 5) and the CALIOP cloud phases obtained for two months, August 2006 and February 2007. We also define the '(quasi-) spherical particle fraction' (*SPF*) in clouds as the ratio of the number of pixels identified as spherical particles to the number of total cloud pixels except those flagged uncertain. By the definition, it is noted that the change in *SPF* is essentially the same as the change in the mass fraction of (quasi-)spherical particles that are commonly used in models. Our results show casual correlations that the *SPF* calculated from the two sensors are very close; on average, the MODIS retrievals and the corresponding CALIOP retrievals

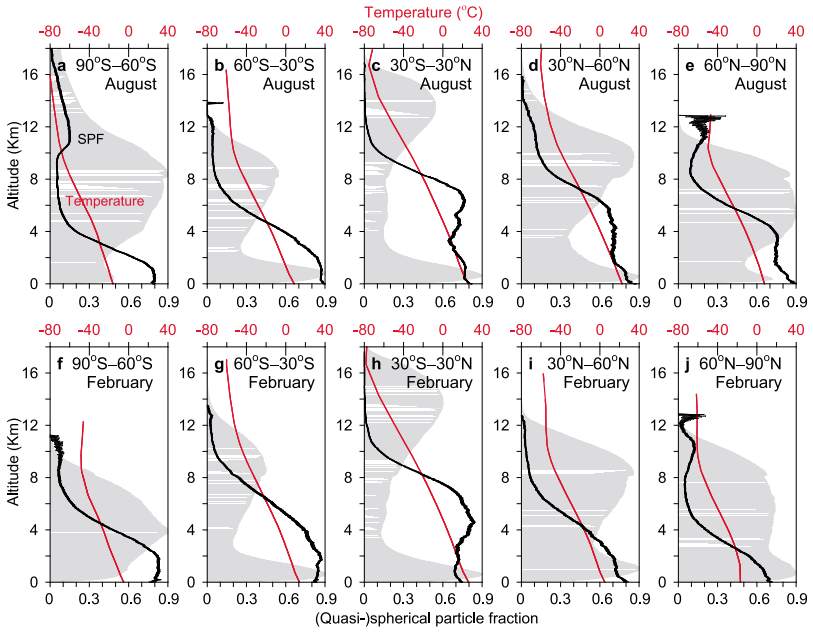

Figure 2. Zonal-mean vertical profiles of (quasi-)spherical particle fraction (black line), temperature (red line), and relative frequency of clouds (gray shade) from the CALIOP data for (a–e) August 2006 and (f–j) February 2007. The standard error of spherical particle fraction is superimposed on the mean profile.

at the CALIOP-detectable cloud tops correlate within about 10% discrepancy.

3. SPF-Temperature Relation in MODIS and CALIOP

[8] The MODIS cloud particle shapes and the independently retrieved collocated cloud-top temperatures are examined first. The MODIS cloud-top temperatures are currently retrieved by a CO_2 slicing method that allows the estimation even for optically thin cirrus clouds [*Menzel et al.*, 2006]. Thus, the minimum detectable value of optical depth for the MODIS cloud-top temperature retrievals (around 0.1) may be different from that for the MODIS IR cloud phase retrievals (around 2.0) [*Choi et al.*, 2005]. The resultant errors may be smoothed out in the averaging processes, however. For June–July–August (JJA), over most of the tropics and Northern Hemisphere, *SPF* values exceed 0.5 (Figure 1a) with relatively small values (less than 0.3) occurring over the tropical deep convection regions, Greenland, and Antarctica. Similar distributions are also observed in the cloud-top temperatures (Figure 1b).

[9] The results in Figures 1a and 1b indicate that *SPF* varies closely with cloud-top temperatures. Figure 1c presents the *SPF*-temperature relationship constructed by taking the daily grid-mean temperature values below 0°C. The mean *SPF* value is calculated for each corresponding temperature bin of 1°C interval, and the standard error of the mean *SPF* is generally less than 0.001. The mean *SPF* at 0°C is less than unity probably because of the sub-grid scale variability in the retrieved cloud phase. This also suggests about 10% of potential uncertainty in the current *SPF* values. The resulting *SPF* increases with increasing temperature at all latitudes. In particular, *SPF* increases rapidly with increasing temperature in the temperature range between −30°C and −10°C. Note that *SPF* of 0.5 at −20°C implies a high degree of heterogeneous ice nucleation in natural clouds globally at the temperature in question [*Pruppacher and Klett*, 1997].

[10] It is intriguing that *SPF* remains above 0.3 at −30°C and 0.1 at −40°C. Based on previous *in situ* observations, these significant *SPF* may be caused by quasi-spherical ice particles, not supercooled liquid particles. For example, *Black and Hallett* [1986] documented the presence very little supercooled water above the −5°C level in hurricanes. *Stith et al.* [2002] reported no substantial supercooled water above the −12°C level, and that the highest level where a trace of supercooled water was observed is at −18°C in the tropics near Kwajalein. Indeed, most *in situ* measurements so far could find only quasi-spherical ice particles with no/negligible supercooled liquid particles at such cold temperatures [*Stith et al.*, 2002; *Korolev and Isaac*, 2003; *Baker and Lawson*, 2006; *Lawson et al.*, 2006, 2008]. In the analysis for the December–January–February (DJF) periods of the same years (Figures 1d and 1e), a clear hemispheric reversal in *SPF* is shown according to the seasonal shift (Figure 1a versus Figure 1d). However, the relationship between the *SPF* and temperature in DJF is similar to that of JJA (Figure 1c versus Figure 1f).

[11] The *SPF* for CALIOP was calculated for individual cloud layers (Figure 2). The temperature profile has been obtained by converting the CALIOP-measured geometrical cloud heights using the National Centers for Environmental Prediction–National Center for Atmospheric Research reanalysis-2 data that cover the entire globe at a 2.5° × 2.5° horizontal resolution (available from http://cdc.noaa.gov). The reanalysis data are used only as a reference for temperature-height relation, and the temperature profile is essentially determined by the CALIOP-observed cloud height. Results show that a considerable amount of spherical particles at very cold temperatures occur throughout cloud layers, not only at the top of clouds. For all cases during

August 2006 (Figures 2a–2e), *SPF* rapidly decreases with increasing altitude (i.e., decreasing temperature) within the range where temperature varies between −10°C and −30°C. *SPF* is near 0.5 at −20°C, which is comparable with the MODIS data, and is up to 0.3 at −30°C. Even larger *SPF* values are found at the level colder than −30°C in the high latitudes (Figures 2a and 2e). The altitude at which cloud layers are most frequent also varies according to latitudes (gray shade in Figure 2). Noticeable *SPF* values are also found in these altitude ranges of very cold temperatures; the corresponding cloud amounts need to be considered for the impact of (quasi-)spherical particles on radiative transfer.

[12] A hemispheric reversal of the August feature is observed in February 2007 (Figures 2f–2j). The well-identified polar stratospheric clouds over the high latitudes in the Southern Hemisphere during August are absent during February (Figure 2a versus Figure 2f). A comparison of the results for February and August shows that the overall relationship between the retrieved *SPF* and the temperature is nearly invariant, except the long tail of the distribution of the spherical particle fraction in very cold temperature ranges (or in the upper troposphere). It is also noted that determining the cloud particle shape near the base of opaque clouds by CALIOP retrievals is limited by the attenuation of a lidar return signal [*Liu et al.*, 2005]; this results in the *SPF* value of less than unity near the surface level. This error, however, may not affect the present results since it occurs at very warm temperatures.

4. Discussions and Summary

[13] The MODIS and CALIOP sensors retrieve the same cloud fields almost simultaneously using completely different measurement and retrieval methods. The *SPF* values from the two independent retrievals correlate within 10% difference on average. It is noted that the present results are comparable with other satellite retrievals. For example, the Polarization and Directionality of the Earth Reflectances (POLDER-1) measurements that flag roughly 10% of clouds as spherical particles in the temperature range −50°C and −40°C [*Doutriaux-Boucher and Quaas*, 2004; *Weidle and Wernli*, 2008]. Therefore, the relationship between *SPF* and temperature found in this study may not be an artifact of the retrieval errors.

[14] This paper presents, based on the satellite observations, that the spherical or quasi-spherical particles may be present in significant amounts at very cold temperatures. It is important to question that what we see from space is clearly differentiated from the image from *in situ* measurements. Theoretical and empirical studies show that water drops are rapidly glaciated to practically negligible amounts below −20°C and hardly exist in natural clouds below −40°C due to homogeneous ice nucleation [*Pruppacher and Klett*, 1997]. Thus, the considerable *SPF* even below −20°C in satellite observations necessarily indicates the large amount of quasi-spherical ice particles (that is used to indicate any small, frozen, droxtal- or spheroid-shaped ice particles), nitric acid compounds, etc.

[15] Recent observations show that quasi-spherical ice particles are characteristically smaller than about 50 μm [*Korolev and Isaac*, 2003]. The small quasi-spherical ice particles actually have optical properties that can lead to confusion with spherical particles in the remote retrievals [*Yang et al.*, 2005; *Zhang et al.*, 2004]. Quantitative issues of these particles remain to be investigated [*Heymsfield*, 2007; *Jensen et al.*, 2009]. However, in many recent *in situ* observations, it has been identified the presence of a considerable amount of quasi-spherical particles in mid- and upper-tropospheric ice clouds (with temperatures < −35°C), including midlatitude wave clouds [*Baker and Lawson*, 2006], midlatitude cirrus clouds [*Lawson et al.*, 2006], extratropical convective clouds [*Stith et al.*, 2002], midlatitude and polar stratiform ice clouds [*Korolev and Isaac*, 2003], and subvisible cirrus clouds in the tropical tropopause layer [*Lawson et al.*, 2008].

[16] Supercooled ternary solutions (HNO_3-H_2SO_4-H_2O) might be a possibility because it would remain spherical in polar stratospheric clouds and in tropical upper tropospheric clouds where temperatures are well below −40°C [*Liu et al.*, 2005]. *Noel et al.* [2008] claimed that the solutions might comprise over 20% of polar stratospheric clouds in the southern hemispheric winter, although this result could be somewhat overestimated due to uncertainty in CALIOP data (D. Winker, personal communication, 2009).

[17] Do the satellite snapshots capture frozen spheres that have not developed crystalline faces? Only a couple of previous cloud chamber experiments found that frozen spheres can exist in a stable state down to −65°C or −70°C [*Mason*, 1952; *Madonna et al.*, 1961]. However, current understanding is that such frozen spheres are likely to exist only in rare quantities in nature, since water drops that freeze in supercooled clouds will either grow rapidly (in seconds) to non-spherical shapes, or freeze homogeneously at about −37°C, which typically produces facets on the frozen drops, which are not perfectly spherical. If the drops do freeze homogeneously into perfect spheres, then subsequent growth in an ice-saturated environment will likely produce non-spherical particles [*Pruppacher and Klett*, 1997].

[18] Do the satellite snapshots capture newly condensed liquid droplets in cumulus updrafts? The odds for these liquid particles to constitute the *SPF* averaged over the large area and the season is very small, because these liquid particles in most *in situ* measurements are associated with ultra-strong convective updraft regions that are of extremely small spatial extent [*Rosenfeld and Woodley*, 2000]. As *Korolev and Isaac* [2003] stated, this question, however, cannot be answered unequivocally with the current aircraft instrumentation because there are no probes that can discriminate between small spherical ice and liquid droplets.

[19] The exact processes and the true composition of the spherical particles in these satellite retrievals need closer scrutiny against *in situ* measurements. Regardless of the nature of these alternatives, the radiative properties of quasi-spherical particles are different from non-spherical particles [*Liou*, 2002; *Yang et al.*, 2005]; thus, the calculation of cloud radiative properties in very cold temperature range currently used in climate models may need to be modified to account for the contribution of the quasi-spherical particles.

[20] In most of today's climate models, cloud particles are generally partitioned into spherical and non-spherical particles based on grid point temperatures on the basis of a threshold temperature. For example, spherical and non-spherical particles in the temperature range above 0°C and below −40°C (or even below −15°C), respectively, and mixed clouds in the temperature range between them [*Del*

Genio et al., 1996]. These assumptions may ignore the possible impact of quasi-spherical particles in cold temperature ranges. Even if the observed *SPF* below −40°C found in this study is neglected (<0.1), the model assumption of complete glaciations of clouds below −20°C may lead to significant underestimation of *SPF* by about 0.4 at −20°C. Based on the different phase function between (quasi-)spherical particles and non-spherical particles [*Liou*, 2002; *Yang et al.*, 2005], the anticipated biases in calculating atmospheric radiative transfer in climate models may not be trivial. The possible effects of the underestimation of *SPF* may be mainly on the cloud optical thickness and shortwave cloud forcing. As a future study, currently used cloud particle shape partitioning schemes need to be re-examined in this respect.

[21] **Acknowledgments.** This research was supported by Cater 2006-4204, DOE grant DE-FG02-01ER63257 and the UC-Lab project "Enhancing California's water management decision support system". The MODIS and CALIOP data were obtained from LAADS and ASDC, respectively. The authors thank K. N. Liou, D. Winker, E. Jensen, B. Kaercher, B. Stevens, S. Ou, and two anonymous reviewers for valuable comments.

References

Baker, B. A., and R. P. Lawson (2006), In situ observations of the microphysical properties of wave, cirrus, and anvil clouds. Part I: Wave clouds, *J. Atmos. Sci.*, *63*, 3160–3185, doi:10.1175/JAS3802.1.

Baum, B. A., P. F. Soulen, K. I. Strabala, M. D. King, S. A. Ackerman, W. P. Menzel, and P. Yang (2000), Remote sensing of cloud properties using MODIS airborne simulator imagery during SUCCESS: 2. Cloud thermodynamic phase, *J. Geophys. Res.*, *105*, 11,781–11,792, doi:10.1029/1999JD901090.

Black, R. A., and J. Hallett (1986), Observations of the distribution of ice in hurricanes, *J. Atmos. Sci.*, *43*, 802–822, doi:10.1175/1520-0469(1986)043<0802:OOTDOI>2.0.CO;2.

Choi, Y.-S., C.-H. Ho, and C.-H. Sui (2005), Different optical properties of high cloud in GMS and MODIS observations, *Geophys. Res. Lett.*, *32*, L23823, doi:10.1029/2005GL024616.

Del Genio, A. D., M.-S. Yao, W. Kovari, and K. K.-W. Lo (1996), A prognostic cloud water parameterization for global climate models, *J. Clim.*, *9*, 270–304, doi:10.1175/1520-0442(1996)009<0270:APCWPF>2.0.CO;2.

Doutriaux-Boucher, M., and J. Quaas (2004), Evaluation of cloud thermodynamic phase parameterizations in the LMDZ GCM by using POLDER satellite data, *Geophys. Res. Lett.*, *31*, L06126, doi:10.1029/2003GL019095.

Fu, Q. (1996), An accurate parameterization of the solar radiative properties of cirrus clouds for climate models, *J. Clim.*, *9*, 2058–2082, doi:10.1175/1520-0442(1996)009<2058:AAPOTS>2.0.CO;2.

Heymsfield, A. J. (2007), On measurements of small ice particles in clouds, *Geophys. Res. Lett.*, *34*, L23812, doi:10.1029/2007GL030951.

Ho, C.-H., M.-D. Chou, M. Suarez, and K.-M. Lau (1998), Effect of ice cloud on GCM climate simulations, *Geophys. Res. Lett.*, *25*, 71–74, doi:10.1029/97GL03356.

Hu, Y. X., et al. (2009), CALIPSO/CALIOP cloud phase discrimination algorithm, *J. Atmos. Oceanic Technol.*, *26*, 2293–2309, doi:10.1175/2009JTECHA1280.1.

Jensen, E. J., et al. (2009), On the importance of small ice crystals in tropical anvil cirrus, *Atmos. Chem. Phys.*, *9*, 5519–5537.

Korolev, A., and G. Isaac (2003), Roundness and aspect ratio of particles in ice clouds, *J. Atmos. Sci.*, *60*, 1795–1808, doi:10.1175/1520-0469(2003)060<1795:RAAROP>2.0.CO;2.

Lawson, R. P., B. Baker, B. Pilson, and Q. Mo (2006), In situ observations of the microphysical properties of wave, cirrus, and anvil clouds. Part II: Cirrus clouds, *J. Atmos. Sci.*, *63*, 3186–3203, doi:10.1175/JAS3803.1.

Lawson, R. P., et al. (2008), Aircraft measurements of microphysical properties of subvisible cirrus in the tropical tropopause layer, *Atmos. Chem. Phys.*, *8*, 1609–1620.

Liou, K. N. (2002), Presentation of a unified theory for light scattering by ice crystals, in An Introduction to Atmospheric Radiation, 2nd ed., pp. 228–231, Elsevier, New York.

Liu, Z., A. H. Omar, Y. Hu, M. A. Vaughan, and D. M. Winker (2005), Part 3: Scene classification algorithms, in *CALIOP Algorithm Theoretical Basis Document*, *PC-SCI-202*, 56 pp., Langley Res. Cent., Hampton, Va.

Madonna, L. A., C. M. Sciulli, L. N. Canjar, and G. M. Pound (1961), Low-temperature cloud-chamber studies on water vapour, *Proc. Phys. Soc.*, *78*, 1218–1222, doi:10.1088/0370-1328/78/6/317.

Mason, B. J. (1952), The spontaneous crystallization of supercooled water, *Q. J. R. Meteorol. Soc.*, *78*, 22–27, doi:10.1002/qj.49707833503.

Menzel, W. P., R. A. Frey, B. A. Baum, and H. Zhang (2006), Cloud top properties and cloud phase, *NASA Algorithm Theor. Basis Doc. ATBD-MOD-04*, 56.

Noel, V., A. Hertzog, H. Chepfer, and D. M. Winker (2008), Polar stratospheric clouds over Antarctica from the CALIPSO spaceborne lidar, *J. Geophys. Res.*, *113*, D02205, doi:10.1029/2007JD008616.

Pruppacher, H., and J. Klett (1997), *Microphysics of Clouds and Precipitation*, Kluwer Acad., Dordrecht, Netherlands.

Rosenfeld, D., and W. L. Woodley (2000), Deep convective clouds with sustained supercooled liquid water down to −37.5°C, *Nature*, *405*, 440–442, doi:10.1038/35013030.

Senior, C. A., and F. B. Mitchell (1993), Carbon dioxide and climate: The impact of cloud parameterization, *J. Clim.*, *6*, 393–418, doi:10.1175/1520-0442(1993)006<0393:CDACTI>2.0.CO;2.

Stith, J. L., J. E. Dye, A. Bansemer, A. J. Heymsfield, C. A. Grainger, W. A. Peterson, and R. Cifelli (2002), Microphysical observations of tropical clouds, *J. Appl. Meteorol.*, *41*, 97–117, doi:10.1175/1520-0450(2002)041<0097:MOOTC>2.0.CO;2.

Storelvmo, T., J. E. Kristjánsson, and U. Lohmann (2008), Aerosol influence on mixed-phase clouds in CAM-Oslo, *J. Atmos. Sci.*, *65*, 3214–3230, doi:10.1175/2008JAS2430.1.

Weidle, F., and H. Wernli (2008), Comparison of ERA40 cloud top phase with POLDER-1 observations, *J. Geophys. Res.*, *113*, D05209, doi:10.1029/2007JD009234.

Yang, P., et al. (2005), Scattering and absorption property database for nonspherical ice particles in the near- through far-infrared spectral region, *Appl. Opt.*, *44*, 5512–5523, doi:10.1364/AO.44.005512.

Zhang, Z., et al. (2004), Geometrical-optics solution to light scattering by droxtal ice crystals, *Appl. Opt.*, *43*, 2490–2499, doi:10.1364/AO.43.002490.

Y.-S. Choi and R. S. Lindzen, Department of Earth, Atmospheric and Planetary Sciences, Massachusetts Institute of Technology, Cambridge, MA 02139, USA.

C.-H. Ho, School of Earth and Environmental Sciences, Seoul National University, Seoul 151-747, South Korea. (hoch@cpl.snu.ac.kr)

J. Kim, Department of Atmospheric and Oceanic Sciences, University of California, Los Angeles, CA 90095, USA.